■ Magnetic Wheels

Combining Complementary Ligands into one Framework for the Construction of a Ferromagnetically Coupled [Mn$^{III}_{12}$] Wheel

Sergio Sanz,[a] Jamie M. Frost,[a] Thayalan Rajeshkumar,[b] Scott J. Dalgarno,[c] Gopalan Rajaraman,*[b] Wolfgang Wernsdorfer,[d] Jürgen Schnack,*[e] Paul. J. Lusby,[a] and Euan K. Brechin*[a]

Abstract: Phenolic oxime and diethanolamine moieties have been combined into one organic framework, resulting in the formation of a novel ligand type that can be employed to construct a rare and unusual dodecametallic Mn wheel, within which nearest neighbours are coupled ferromagnetically.

The success with which coordination chemists have produced molecules with fascinating physical properties is derived from a systematic exploration of the effects of ligand design, metal identity and heating regime upon cluster symmetry, topology and nuclearity.[1] Past successes and future progress are underpinned by judicious ligand design, looking not only at the way in which ligands can bridge between metal centres, but also how the periphery can be derivatized to enhance, for example, solubility, substrate specificity, post-synthetic modification or magnetic exchange.[2] Two families of ligands that have had enormous success in the construction of Mn cluster compounds in particular are the phenolic oximes[3] and the diols.[4] The former tend to construct clusters based on the triangular [Mn$_3$O(R-sao)$_3$]$^+$ (saoH$_2$ = salicylaldoxime) building block, at least in alcohol, whereas the latter have more structural flexibility and have demonstrated a wide variety of coordination modes (from μ- to μ$_5$-bridging), but they are often observed to impart a degree of curvature that can result in the formation of molecular wheels.[4a] Wheels have long fascinated chemists, partly due to their beautiful structural aesthetics, but also because they possess inherently fascinating physics.[5] They are model compounds for the study of quantum effects and spin frustration, and have been proposed as candidates for quantum-information processing.[5] Transition-metal-based wheels can be singly or multiply stranded, the former describing linked monometallic fragments,[6] and the latter linked polymetallic fragments or layered complexes, in which two or more wheels run in parallel.[7]

One common approach for making Mn clusters is to use two ligand types in one-pot serendipitous self-assembly. This is especially fruitful if the ligands have a track record of success in making Mn clusters in their own right, and if the respective building blocks are complementary. Indeed our initial attempts at employing phenolic oximes and diols in the same reactions has proved to be somewhat successful.[8] An alternative ap-
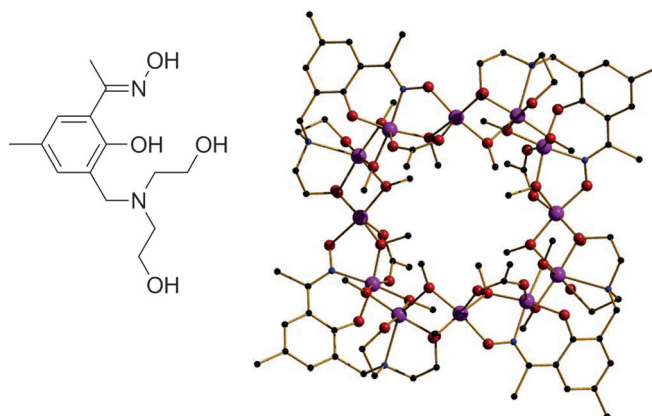
[a] Dr. S. Sanz, J. M. Frost, Dr. P. J. Lusby, Prof. E. K. Brechin
EaStCHEM School of Chemistry, The University of Edinburgh
West Mains Road, Edinburgh, EH9 3JJ (UK)
E-mail: ebrechin@staffmail.ed.ac.uk

[b] T. Rajeshkumar, Dr. G. Rajaraman
Department of Chemistry, Indian Institute of Technology Bombay
Powai, Mumbai 400 076 (India)
E-mail: rajaraman@chem.iitb.ac.in

[c] Dr. S. J. Dalgarno
Institute of Chemical Sciences, Heriot-Watt University
Riccarton, Edinburgh, Scotland, EH14 4AS (UK)

[d] Dr. W. Wernsdorfer
Institut Néel, 25 Avenue des Martyrs, BP 166
38042 Grenoble, Cedex 9 (France)

[e] Prof. J. Schnack
Universität Bielefeld, Fakultät für Physik
Postfach 100131, 33501 Bielefeld (Germany)
E-mail: jschnack@uni-bielefeld.de

⌨ Supporting information for this article is available on the WWW under
http://dx.doi.org/10.1002/chem.201304740.

Figure 1. Left: Structure of the pro-ligand H$_4$L. Right: Molecular structure of **1**: Mn = purple, O = red, N = blue and C = black; hydrogen atoms and some carbon atoms are omitted for clarity.

proach would be to combine the phenolic oxime and diol moieties within the same ligand framework, and herein, we report the synthesis, structure and magnetic properties of the dodecametallic wheel [Mn$^{III}_{12}$(OMe)$_{16}$(L)$_4$(O$_2$CCMe$_3$)$_4$(MeOH)$_4$] (**1**) constructed by using the new pro-ligand H$_4$L (Figure 1, left).

Reaction of MnCl$_2$·4H$_2$O, H$_4$L and Me$_3$CCO$_2$Na in a basic MeOH solution resulted in the formation of black rod-like crystals after slow evaporation of the filtered mother liquor, after
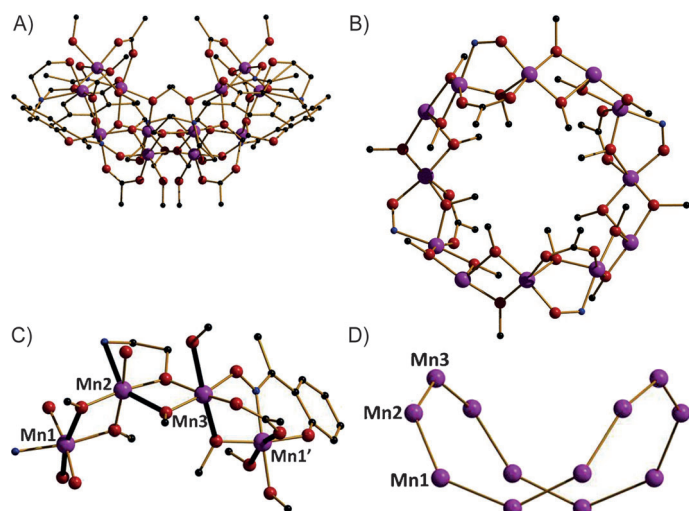
Figure 2. A) Molecular structure of **1** highlighting the saddle shape. Hydrogen atoms and some carbon atoms are omitted for clarity. B) Magnetic core of **1**. C) Three different exchange interactions between the Mn centres; Mn1–Mn2 = J_1, Mn2–Mn3 = J_2 and Mn3–Mn1' = J_3. The solid black lines show the Jahn–Teller axes of the Mn^{III} ions. D) Metallic skeleton of **1**: Mn = purple, O = red, N = blue and C = black.

five days (for details, see the Supporting Information). The crystals were found to be in a tetragonal crystal system and structure solution was performed in the $I4_1/a$ space group. The structure describes a saddle-like or basket-shaped, single-stranded dodecametallic wheel (Figures 1 and 2). The four symmetry-equivalent L^{4-} ligands bridge a total of four Mn ions: the oximic and phenolic moieties are μ-bridging (Mn-N-O-Mn 22.76°) and terminally bonded (Mn—O 1.873 Å), respectively, and the two alkoxide arms of the diethanolamine do likewise, one terminally bonded (Mn—O 1.903 Å) and one μ-bridging (Mn—O 1.958 Å; Mn-O-Mn 106.6°). The sixteen MeO⁻ ions and four carboxylates are all μ-bridging (Mn—O(Me) 1.882–2.157; Mn-O(Me)-Mn 101.08–104.86°), and the four MeOH molecules are terminally bonded to Mn3 and symmetry equivalents (Mn—O 2.287 Å). The magnetic core of the molecule can thus be described as consisting of three basic units: Mn1–Mn2 bridged by two methoxides, Mn2–Mn3 bridged by one methoxide and one alkoxide from the diethanolamine moiety; and Mn3–Mn1' by one methoxide, one carboxylate and one oximic NO moiety (Figure 2 c). The metallic wheel is approximately 9 Å in diameter (Mn3⋯Mn3'). There are no intra- or intermolecular hydrogen bonds, with the closest intermolecular interactions being between the methoxides and the Ph ring of the L^{4-} ligand (C-(OMe)⋯C$_{(ring)}$ 3.311 Å) and this causes the molecules to pack in an aesthetically pleasing head-to-tail arrangement (Figure S1 in the Supporting Information).

A search of the Cambridge structural database (CSD) reveals only three examples of dodecametallic Mn wheels in the literature: the metalladiazamacrocycle [Mn₁₂(tpeshz)₁₂(dmf)₁₂] (H₃tpeshz = N-trans-2-pentenoylsalicylhydrazide),[9] the mixed-valent [$Mn^{III}_6Mn^{II}_6$(O₂CR)₁₄(L)₈] (LH₂ = N-alkyldiethanolamine), in which Mn^{III} and Mn^{II} ions alternate around a chair-like wheel,[10] and the recently published mixed-valent "triangular" wheel [$Mn^{II}_6Mn^{III}_6$(mpt)₆(CH₃CO₂)₁₂(py)₆] (H₃mpt = methyl-1,3,5-penta-
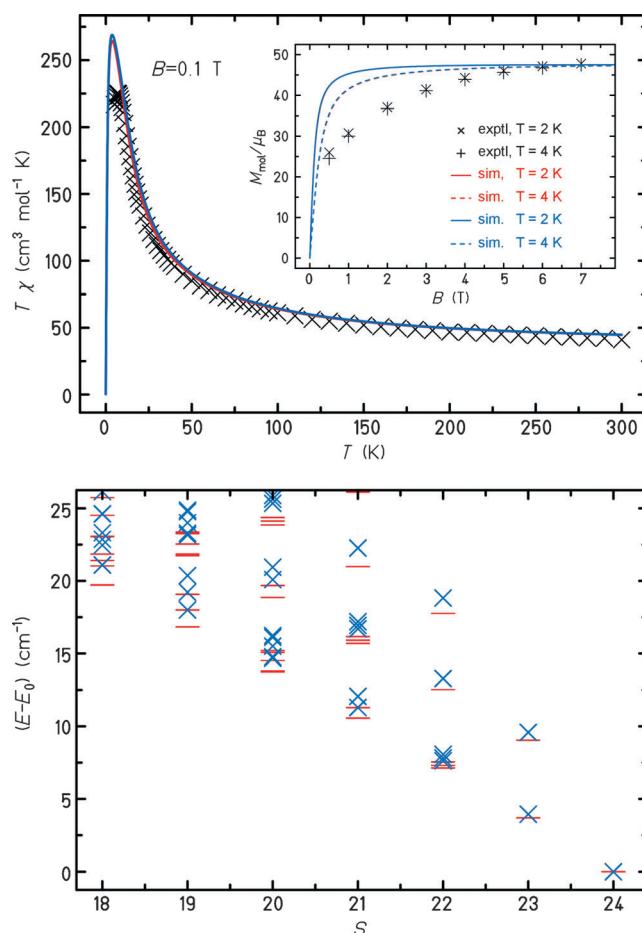

Figure 3. Top: plot of the χT product versus temperature for complex **1** in an applied field of 0.1 T. The black crosses are the experimental data, the blue line is a simulation with the $3J$ nearest-neighbour model and the red line is a simulation with the full $9J$ model. Bottom: energy versus total spin state for the lowest lying S levels derived from the isotropic simulation of the susceptibility. Blue crosses are from the $3J$ model, red lines are from the $9J$ model.

netriol) consisting of alternating homovalent [Mn^{II}_2] and [Mn^{III}_2] dimers.[10g] Interestingly, the saddle-like topology seen in **1** is rather reminiscent of the mixed-valent wheel [$Mn^{III}_8Mn^{II}_8$-(O₂CMe)₁₆(teaH)₁₂] built using the closely related ligand triethanolamine (teaH₃).[6] No magnetic data were reported for the [Mn^{III}_{12}] complex, and both mixed-valent species display dominant antiferromagnetic exchange interactions.

The magnetic susceptibility (χ) of **1** was measured from 300 to 5 K in an applied field of 0.1 T, and the results are plotted as the χT product versus T in Figure 3. The χT value of approximately 41 cm³ K mol⁻¹ at 300 K is above that expected for twelve non-interacting Mn^{III} ions (36 cm³ K mol⁻¹ for g = 2). This value increases steadily as the temperature is decreased, reaching a maximum of 225.4 cm³ K mol⁻¹ at 7.5 K, before dropping slightly to 216.9 cm³ K mol⁻¹ at 5 K. This behaviour suggests dominant ferromagnetic exchange interactions in **1**. The low-temperature magnetisation rises to saturation within 7 T, although the initial slope is much smaller than expected for a Brillouin function, suggesting the presence of sizeable single-ion anisotropy, as might be expected for Mn^{III} (Figure 3). Due

to the huge dimension of the Hilbert space (244,240,625), an exact eigenvalue determination of an anisotropic spin Hamiltonian is impossible, and thus we have performed DFT calculations (see the Supporting Information) to determine the pertinent exchange parameters, which we then employ in a spin Hamiltonian (Table S1 in the Supporting Information).[11]

In complex **1** there are three unique nearest-neighbour (1,2) interactions: Mn1–Mn2 (J_1), Mn2–Mn3 (J_2) and Mn3–Mn1′ (J_3; Figure 2C and Figure S2 in the Supporting Information). A previous theoretical study of a different [Mn$_{12}$] wheel suggested that both the next-nearest (1,3) and next-next-nearest (1,4) interactions may be non-negligible,[10f] and thus we have also calculated the three (1,3) and three (1,4) interactions. The calculated nearest-neighbour interactions (based on the $\hat{H} = -2\,J_{i,j}\hat{S}_i\hat{S}_j$ formalism) are $J_1 = +11.11$ cm^{-1}, $J_2 = +6.71$ cm^{-1} and $J_3 = +1.90$ cm^{-1}. The interactions are computed to be ferromagnetic in nature, with the magnitude diminishing significantly from $J_1–J_3$. The (1,3) and (1,4) interactions are computed to be much smaller in magnitude and near zero ($J_4 = -0.05$ cm^{-1}, $J_5 = -0.04$ cm^{-1}, $J_6 = -0.04$ cm^{-1}, $J_7 = +0.03$ cm^{-1}, $J_8 = +0.01$ cm^{-1}, $J_9 = -0.07$ cm^{-1}). Therefore, these can be excluded from further discussion.

By using the exchange-interaction parameters extracted from DFT, spin Hamiltonian simulations have been performed for an isotropic spin Hamiltonian, that is, Heisenberg and Zeeman terms, employing the finite-temperature Lanczos method (FTLM), to approximately evaluate the susceptibility and magnetisation.[12] The result for the χT product versus T reproduces the data very well, because χT in the strong exchange limit only very weakly depends on the single-ion anisotropies, and is therefore dominated by the exchange parameters (Figure 3). The influence of antiferromagnetic next-nearest and next-next-nearest neighbour exchange, which in principle could lead to interesting frustrated ferromagnets, is negligible.[13] The low-temperature magnetisation on the contrary depends strongly on anisotropy, and a simulation by using a Heisenberg model gave a much poorer fit (Figure 3). It is clear that the anisotropy term will reduce the magnetisation at low temperatures. Unfortunately, anisotropy breaks the SU(2) symmetry of the Heisenberg model used in our simulations, and programs that could deal with such large systems are not available—the largest anisotropic system simulated to date contains just six Mn^{III} ions and one Cr^{III} ion.[14] Simulations of the magnetisation by using only the ground multiplet (giant-spin approximation) would not give good results since the Heisenberg model simulations show that the low-lying multiplets are nested, with the gap to the first excited state being only 3.5 cm^{-1} (Figure 3), and thus strongly contribute to thermodynamic observables even at the lowest temperatures.

Previous theoretical studies on {Mn^{III}(OR)$_2$Mn^{III}} dimers revealed that the angle between neighbouring Jahn–Teller (JT) axes is crucial in determining the sign and strength of the magnetic interaction.[15] Based on this classification, the nearest-neighbour interactions in **1** all belong to type III (Figure S3 in the Supporting Information), with the angle between JT axes being 87.2 (J_1), 100.9 (J_2) and 126.7° (J_3). When the angle increases, the orthogonality between the two d$_{z^2}$ orbitals is
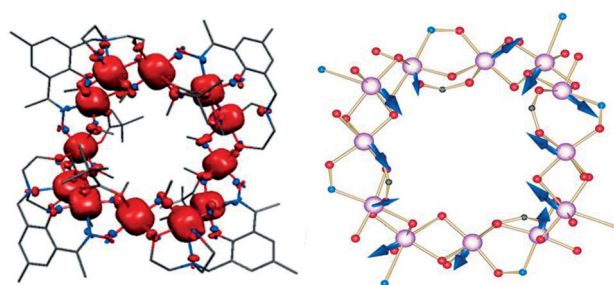

Figure 4. Left: spin-density plot for **1**. Right: D_{zz} orientations of the twelve Mn^{III} ions in **1**.

lifted, and the cross-interaction between the d$_{z^2}$ and the empty d$_{x^2-y^2}$ orbital decreases, leading to a decrease in the strength of the magnetic exchange. The computed exchange interactions and experimentally observed JT angles for **1** thus correlate rather nicely with previously published magneto-structural correlations.[15] The computed spin-density plot of the $S = 24$ state is shown in Figure 4, with a mixture of spin delocalisation (along the JT axes) and spin polarisation observed. Because the JT axes are perpendicular to each other, one of the μ-bridging O-atoms has significant spin density, whereas the other has a very small spin density, and the net spin densities on both decrease when the magnitude of J decreases (Table S2 in the Supporting Information).

We have also computed the single-ion zero-field splitting (ZFS) of the individual Mn^{III} ions by using monomeric models (Table S3 and Figure S4 in the Supporting Information). The computed D_{zz} values are in the range -2.0 to -1.5 cm^{-1}. Although the sign is as anticipated, the magnitudes are a little smaller than that expected[11] for complexes of Mn^{III} and can likely be attributed to the distorted octahedral Mn^{III} coordination environments present in **1**.[16] The computed D_{zz} directions are shown in Figure 4, all being approximately collinear to the JT axes (Table S3 in the Supporting Information). The D_{zz} axes of any two nearest neighbours are approximately perpendicular to each other, and thus the $D_{S=4}$ that arise from each of the twelve dimeric units are expected to be small. Indeed, computed values on selected dimeric models yield $D_{S=4}$ values in the range -0.39 to -0.71 cm^{-1}, and one would expect this to reduce further when the model size increases and reaches [Mn$^{III}_{12}$] (Table S4 and Figure S5 in the Supporting Information).

AC susceptibility measurements showed strong frequency dependence at $T \leq 5$ K; an Arrhenius analysis of the out-of-phase data in combination with DC magnetisation decay data obtained from a single crystal gave $U_{eff}/k_B = 51$ K and $\tau_0 = 3.2 \times 10^{-11}$ s (Figures S6 and S7 in the Supporting Information). A barrier of 51 K is suggestive of a small $D_{(cluster)} \approx 0.06$ cm^{-1}, as was predicted by computation. Single-crystal hysteresis loop measurements performed with the field applied along the easy axis of the molecule show temperature- and sweep-rate dependent signals below approximately 2 K (Figure 5). The loops have no well-defined quantum steps, and thus a rather rounded appearance, as a direct result of the plethora of low-lying excited spin states.

In conclusion, the new pro-ligand H$_4$L, combining phenolic oxime and diethanolamine moieties within the same structural
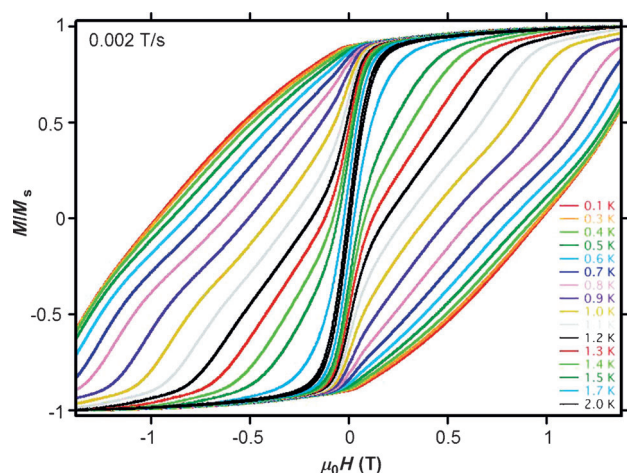
Figure 5. Single-crystal hysteresis-loop measurements for **1** with the field applied along the easy axis of the molecule. The magnetisation is normalised to its saturation value.

framework has led to the isolation of an unusual dodecametallic [Mn$^{III}_{12}$] wheel. Indeed, it is just the fourth [Mn$_{12}$] wheel of any kind, the second homovalent wheel and the first to display ferromagnetic exchange between neighbours leading to a $S = 24$ ground state. These results suggest that pairing complementary ligands into the same organic scaffold may lead to a host of fascinating new structure types.

Acknowledgement

[1] R. E. P. Winpenny in *Comprehensive Coordination Chemistry II, Vol. 7* (Eds.: J. A. McCleverty, T. J. Meyer), Elsevier, Amsterdam, **2004**, Chapter 7.3, pp. 125–175.

[2] a) G. Aromí, E. K. Brechin, *Struct. Bonding (Berlin)* **2006**, *122*, 1; b) M. Murrie, D. J. Price, *Annu. Rep. Prog. Chem.* **2007**, *103*, 20; c) K. S. Murray, *Aust. J. Chem.* **2009**, *62*, 1081; d) R. Bagai, G. Christou, *Chem. Soc. Rev.*

2009, *38*, 1011; e) G. E. Kostakis, I. J. Hewitt, A. M. Ako, V. Mereacre, A. K. Powell, *Phil. Trans. R. Soc. A* **2010**, *368*, 1509.

[3] a) R. Inglis, C. J. Milios, L. F. Jones, S. Piligkos, E. K. Brechin, *Dalton Trans.* **2012**, *41*, 181; b) R. Inglis, L. F. Jones, C. J. Milios, S. Datta, A. Collins, S. Parsons, W. Wernsdorfer, S. Hill, S. P. Perlepes, S. Piligkos, E. K. Brechin, *Dalton Trans.* **2009**, 3403; c) C. J. Milios, S. Piligkos, E. K. Brechin, *Dalton Trans.* **2008**, 1809.

[4] a) A. J. Tasiopoulos, S. P. Perlepes, *Dalton Trans.* **2008**, 5537; b) A. M. Ako, Y. Lan, V. Mereacre, E. Ruiz, D. Aravena, C. E. Anson, A. K. Powell, *Dalton Trans.* **2013**, *42*, 9606; c) R. W. Saalfrank, A. Scheurer, R. Prakash, F. W. Heinemann, T. Nakajima, F. Hampel, R. Leppin, B. Pilawa, H. Rupp, P. Müller, *Inorg. Chem.* **2007**, *46*, 1586; d) R. W. Saalfrank, R. Prakash, H. Maid, F. Hampel, F. W. Heinemann, A. X. Trautwein, L. H. Bottger, *Chem. Eur. J.* **2006**, *12*, 2428.

[5] a) A. Furrer, O. Waldmann, *Rev. Mod. Phys.* **2013**, *85*, 367; b) G. A. Timco, E. J. L. McInnes, R. E. P. Winpenny, *Chem. Soc. Rev.* **2013**, *42*, 1796; c) G. A. Timco, T. B. Faust, F. Tuna, R. E. P. Winpenny, *Chem. Soc. Rev.* **2011**, *40*, 3067; d) P. Santini, S. Carretta, F. Troiani, G. Amoretti, *Phys. Rev. Lett.* **2011**, *107*, 230502.

[6] M. Murugesu, W. Wernsdorfer, K. A. Abboud, G. Christou, *Angew. Chem.* **2005**, *117*, 914; *Angew. Chem. Int. Ed.* **2005**, *44*, 892.

[7] A. J. Tasiopoulos, A. Vinslava, W. Wernsdorfer, K. A. Abboud, G. Christou, *Angew. Chem.* **2004**, *116*, 2169; *Angew. Chem. Int. Ed.* **2004**, *43*, 2117.

[8] M. Manoli, R. Inglis, M. J. Manos, V. Nastopoulos, W. Wernsdorfer, E. K. Brechin, A. J. Tasiopoulos, *Angew. Chem.* **2011**, *123*, 4533; *Angew. Chem. Int. Ed.* **2011**, *50*, 4441.

[9] R. P. John, K. Lee, M. S. Lah, *Chem. Commun.* **2004**, 2660.

[10] a) E. M. Rumberger, L. N. Zakharov, A. L. Rheingold, D. N. Hendrickson, *Inorg. Chem.* **2004**, *43*, 6531; b) E. M. Rumberger, S. J. Shah, C. C. Beedle, L. N. Zakharov, A. L. Rheingold, D. N. Hendrickson, *Inorg. Chem.* **2005**, *44*, 2742; c) S. J. Shah, C. M. Ramsey, K. J. Heroux, A. G. DiPasquale, N. S. Dalal, A. L. Rheingold, E. del Barco, D. N. Hendrickson, *Inorg. Chem.* **2008**, *47*, 9569; d) D. Foguet-Albiol, T. A. O'Brien, W. Wernsdorfer, B. Moulton, M. J. Zaworotko, K. A. Abboud, G. Christou, *Angew. Chem.* **2005**, *117*, 919; *Angew. Chem. Int. Ed.* **2005**, *44*, 897; e) W. Wernsdorfer, T. C. Stamatatos, G. Christou, *Phys. Rev. Lett.* **2008**, *101*, 237204; f) J. Cano, R. Costa, S. Alvarez, E. Ruiz, *J. Chem. Theory Comput.* **2007**, *3*, 782; g) S. Zartilas, C. Papatriantafyllopoulou, T. C. Stamatatos, V. Nastopoulos, E. Cremades, E. Ruiz, G. Christou, C. Lampropoulos, A. J. Tasiopoulos, *Inorg. Chem.* **2013**, *52*, 12070.

[11] a) F. Neese, *J. Am. Chem. Soc.* **2006**, *128*, 10213; b) C. Duboc, D. Ganyushin, K. Sivalingam, M.-N. Collomb, F. Neese, *J. Phys. Chem. A* **2010**, *114*, 10750; c) E. Cremades, S. Gómez-Coca, D. Aravena, S. Alvarez, E. Ruiz, *J. Am. Chem. Soc.* **2012**, *134*, 10532.

[12] a) J. Jaklič, P. Prelovšek, *Phys. Rev. B* **1994**, *49*, 5065; b) J. Schnack, O. Wendland, *Eur. Phys. J. B* **2010**, *78*, 535; c) J. Schnack, P. Hage, H.-J. Schmidt, *J. Comput. Phys.* **2008**, *227*, 4512.

[13] M. Haertel, J. Richter, D. Ihle, J. Schnack, S.-L. Drechsler, *Phys. Rev. B* **2011**, *84*, 104411.

[14] V. Hoeke, M. Heidemeier, E. Krickemeyer, A. Stammler, H. Bögge, J. Schnack, A. Postnikov, T. Glaser, *Inorg. Chem.* **2012**, *51*, 10929.

[15] N. Berg, T. Rajeshkumar, S. M. Taylor, E. K. Brechin, G. Rajaraman, L. F. Jones, *Chem. Eur. J.* **2012**, *18*, 5906.

[16] a) B. J. Kennedy, K. S. Murray, *Inorg. Chem.* **1985**, *24*, 1552; b) S.-W. Hung, F.-A. Yang, J.-H. Chen, S.-S. Wang, J.-Y. Tung, *Inorg. Chem.* **2008**, *47*, 7202; c) J. Krzystek, G. J. Yeagle, J.-H. Park, R. D. Britt, M. W. Meisel, L.-C. Brunel, J. Telser, *Inorg. Chem.* **2003**, *42*, 4610.